



LUND UNIVERSITY
Faculty of Science



Real- and Quasi-Atomic Layer Etching for Ultra-High Resolution Patterning

Yoana Ilarionova

Thesis submitted for the degree of Master of Science
Project duration: 8 months

Supervised by Mohammad Karimi and Ivan Maximov



Department of Physics
Division of Solid State Physics
Spring 2022

**Real- and Quasi-Atomic Layer Etching for
Ultra-High Resolution Patterning**
Master's thesis

Author: Yoana Ilarionova
Supervisors: Mohammad Karimi and Ivan Maximov
Examiners: Claudio Verdozzi and Adam Burke

Spring 2022

Contents

1	Introduction	5
2	Theoretical background	8
2.1	Reactive-ion etching	8
2.2	Atomic layer etching	8
2.3	Adsorption of Cl ₂ on Si(100)	11
3	Experimental tools and conditions	12
3.1	PlasmaTherm ICP-RIE Apex SLR Tool	12
3.2	Cyclic etching process towards atomic layer etching	13
3.3	Sample fabrication	14
3.3.1	Type A - Resist mask	15
3.3.2	Type B - Cr mask with holes	16
3.3.3	Type C - Cr dots mask	16
3.3.4	Type D - SiO ₂ mask	17
3.4	Optical emission spectroscopy	17
3.5	Scanning electron microscope	19
4	Results and discussions	21
4.1	Reference spectra and chamber cleaning	21
4.2	Cyclic etching process and ALE	25
4.2.1	Activation and Cl ₂ purging optimization	26
4.2.2	Finding the ALE window	29
5	Outlook	34

Acknowledgments

I would like to express my gratitude towards a few people I consider very important to me and the project. First of all (in chronological order), Anette L fstrand for suggesting this project - I would not even know about it otherwise.

Second, to all the wonderful people at AlixLabs that have given me the opportunity to do such an amazing project with them. Especially my supervisor Mohammad Karimi for teaching me so much over the course of the project both in terms of the specific process we were trying to achieve and purely practical things like using the tools in the lab, Dmitry Suyatin for his continuous support with the lab equipment and valuable input and Reza Jafari Jam for his help with some of the experiments and ideas in improving some of the processes used in the project. All of the people at AlixLabs have been amazing and it was a pleasure working with them.

Third, to my supervisor Ivan Maximov for his help with the theoretical side of the project and his feedback on the manuscript and the presentation.

And last but most definitely not least, to my dear boyfriend Daniel Nastasijevic for being by my side the entire time.

List of abbreviations

A.U.	arbitrary units	ML	megalangmuir
ALD	atomic layer deposition	MLs	monolayers
ALE	atomic layer etching	ms	millisecond
Ar	argon	mTorr	milliTorr
ARC	anti-reflective coating	MW	microwave
C	degrees Celsius	N ₂	nitrogen (molecular)
C ₂	carbon (molecular)	nm	nanometer
CH ₄	methane	O	oxygen (atomic)
CHF ₃	trifluoromethane	O ₂	oxygen (molecular)
Cl	chlorine (atomic)	OES	optical emission spectroscopy
Cl ₂	chlorine (molecular)	OH	hydroxile group
cm	centimeter	PMGI	poly-methyl glutarimide
CO	carbon monoxide	RF	radio frequency
Cr	chromium	RIE	reactive-ion etching
DC	direct current	rpm	rotations per minute
DTL	displacement Talbot lithography	rpm ²	rotations per minute squared
F	fluorine	s	second
H	hydrogen (atomic)	sccm	standard cubic centimeters per minute
H ₂	hydrogen (molecular)	SEM	scanning electron microscope
HF	hydrofluoric acid	Si	silicon
Hz	hertz	SiCl ₂	silicon dichloride
ICP	inductively coupled plasma	SiO ₂	silicon dioxide
MFC	mass flow controller	UV	ultraviolet
min	minute	W	watt
mJ	millijoule	μm	micrometer

Abstract

An attempt was made at developing atomic layer etching from a cyclic etching process in an ICP-RIE tool. During the process OES was used for contamination monitoring and estimation of the relative amount of Cl_2 left in the chamber during the etch step of cyclic etching processes. The process parameters were then optimized resulting in a quasi-ALE process suitable for pattern transfer as shown by the patterned samples used in the process. Due to the precise control of the etch rate and the smooth etched surface, the optimized process could be applicable for ultra-high resolution patterning.

Chapter 1

Introduction

To satisfy the evergrowing demand for faster and more powerful computers, the production of better processors is a high priority of the semiconductor industry. That would feature putting more and more transistors (the processor's operation units - the more there are, the more powerful the processor is) onto the same space on the chip (even though the chips are slowly increasing too)[\[1\]](#). How is that possible? By making the transistors smaller and smaller[\[2\]](#). That is the reason why once upon a time a computer would take up an entire room and nowadays a phone is a faster and more powerful version that can fit in your pocket while doing much more than what a computer was initially meant to do.

Initially scaling down the transistors was relatively easy, scale the dimensions so that the transistors' properties remain the same and that was enough but as time went on scaling down in the same way became impossible. As the scale approached nanometer, some quantum effects started to affect the transistors' performance and new solutions other than just scaling needed to be found. For example, when the gate oxide needed to become thinner but its dielectric constant was small enough to allow a large amount of electrons to tunnel through at that thickness, the oxide material was changed to reduce the tunneling.

Fabricating transistors or any similar structures happens with three main methods - etching, deposition and lithography. Usually, there is a sample to work on and a final product in mind. While getting from the sample to the end product, it may be necessary to remove material from the sample, also known as etching, or add a different material - deposition. However, these techniques by themselves can only manipulate whole layers of the material. If there is a particular structure that is to be fabricated, it needs to be patterned - that usually features the deposition of a material that is easily manipulated, e.g. photoresist - it can be manipulated with light, then the pattern can either be "drawn" on it, e.g. by a laser or an electron beam, or be transferred from a template mask. The former approach is more often used in process development since it usually takes a long time to complete such a pattern or in template mask fabrication. The latter approach is used when the same pattern is used many times. Moreover, when the lithography

is done, the pattern needs to be transferred to the sample. The pattern transfer could be subtractive - the pattern is etched into the material under the mask or additive - material could be deposited over the patterning layer and the resulting pattern would be the negative of the initial one.

Patterning can be done in many ways. One of the most common ones is photolithography - a photoresist is deposited on the sample and exposed to light shining through a template mask, then the resist is developed and it has the desired pattern. In a similar manner an electron beam or a photon beam can "draw" the pattern on the appropriate resist material instead of using a template mask.

When it comes to deposition, material could be evaporated on the sample, either by evaporating the source material thermally or by using an electron beam, or sputtered (when plasma knocks out atoms or ions of a target material to have them redeposited on the sample). Moreover, material could be grown on top of the sample via chemical vapor deposition. In particular, some chemicals can saturate the sample surface and after they react with another gas (typically water vapor), leave exactly one atomic layer of material grown on the sample - this type of process is known as atomic layer deposition (ALD) and using it would ensure high degree of control of the deposited material's thickness.

In terms of etching, there are wet etching and dry etching techniques. Wet etching feature immersing the sample in a solution that can react with the material that needs to be etched and remove it. It is purely chemical etching but usually results in isotropic removal of material and lacks resolution. However, if the process requires directional etching, reactive ion etching can be used. It features chemically reactive ions being accelerated towards the sample and removing material. This type of etching is both physical and chemical and depending on the process parameters could be both directional or isotropic or in-between - it removes material in all directions but removes more in a certain direction, e.g. it may remove more material in the downwards direction (towards the sample) while removing half as much material in the direction perpendicular to it (parallel to the sample surface).

Out of all etching techniques, reactive ion etching (RIE) has been widely used in the semiconductor industry due to its anisotropy. However, with the transistors shrinking in size in the recent years, RIE does not offer sufficient control of the etch rate, which is a problem if the features being etched are shallow enough to be comparable to the minimal amount of RIE that can be achieved consistently. Atomic layer etching (ALE) is an alternative that ideally etches the substrate one layer at a time and the superior control of the etching depth makes it ideal for etching shallow features demanding great precision. In addition, ALE is known to smoothen the surface of the etched material making it suitable for high-resolution patterning.

The first known ALE process has been described in a patent^[3] by Max N. Yoder published 1988. The patent features a tool for ALE of diamond and the recipe it was meant to use for the process. In the following years ALE of other materials has been reported, such as gallium arsenide (1989^[4]), silicon (1990^[5]), and silicon dioxide (1994^[6]).

The underlying principle of ALE is modifying the substrate surface and removing only the modified layer. A process gas has been specifically chosen so when bound to a

substrate atom, the energy needed to remove said atom is lower than it was without the bound process gas. The process gas is introduced into the chamber so it can bind to the top layer of the sample or in other words activate the surface. Then the remaining gas is purged and inert ions are accelerated towards the substrate with just enough energy to assist the removal of the top layer but not enough to disturb the rest of the structure, i.g. knock an additional atom that was not activated or displace an atom in the substrate lattice. After the plasma has had the chance to remove the activated surface completely, the plasma generation is stopped and the remnants of the plasma are purged.

In literature, it is often discussed whether a certain process is pure ALE or quasi-ALE. If ALE is the only etching process happening, then the process is considered pure ALE. However, in many cases there may be sputtering during the etch step or chemical etching removal in the activation step that can contribute to the etching in addition to the ALE. Such processes are known as quasi-ALE.

The aim of this thesis is the development of ALE using the PlasmaTherm Cl-Apex ICP-RIE tool(see section [3.1](#)). That consists of finding the suitable parameters and evaluating whether the developed process is real or quasi-ALE by testing the known characteristics of the process. In addition, chamber cleanliness and its influence were investigated since the tool is also used for processes that may contaminate the chamber and thus, affecting the ALE process. Optical emission spectroscopy was used to monitor plasma content and relative concentration of species.

Chapter 2

Theoretical background

2.1 Reactive-ion etching

In reactive-ion etching, a widely used dry etching technique, plasma containing atoms, radicals and chemically reactive ions is used to remove material from a sample surface. The ions are created in the tool chamber supplied with a process gas (or gas mixture), which has the plates of a huge capacitor at the top and the bottom. The top one is typically connected to a source of radio-frequency voltage (RF source) while the bottom one is grounded. The changing potential of the top plate is sufficient to attract some electrons from the gas particles ionizing them. The RF voltage also creates a potential difference (DC bias) which accelerates the ions towards the grounded plate. If the power of the RF source commonly referred to as RF power is bigger, so is the DC bias and in turn the energy of the ions. In that case, the ions can physically etch material (sputtering) in addition to the reactive removal. The pressure also affects the isotropy of the etching - the lower the pressure the more isotropic the etch; the higher the pressure the more directional the etch.

2.2 Atomic layer etching

Similar to ALD, which deposits one atomic layer at a time, ALE is an etching process that removes one atomic layer at a time. That is possible if the material to be etched is exposed to a suitable process gas that reduces the energy needed to remove one surface atom by binding to said atom (see fig.2.1). This step is called surface activation. For example, in this project the material etched is Si and the process gas is Cl_2 . A Si atom needs 4.7 eV of energy to be removed from the surface[7], while SiCl_2 would need about 2.3 eV of energy to leave the surface[8].

The additional energy for atom removal could be provided by different means, e.g. thermally[9, 10], by photons[11], by electron-beam generated plasma[12], by neutral beam[13] or by the means of inert ions[14]. In this project, Ar ions are used to supply the additional

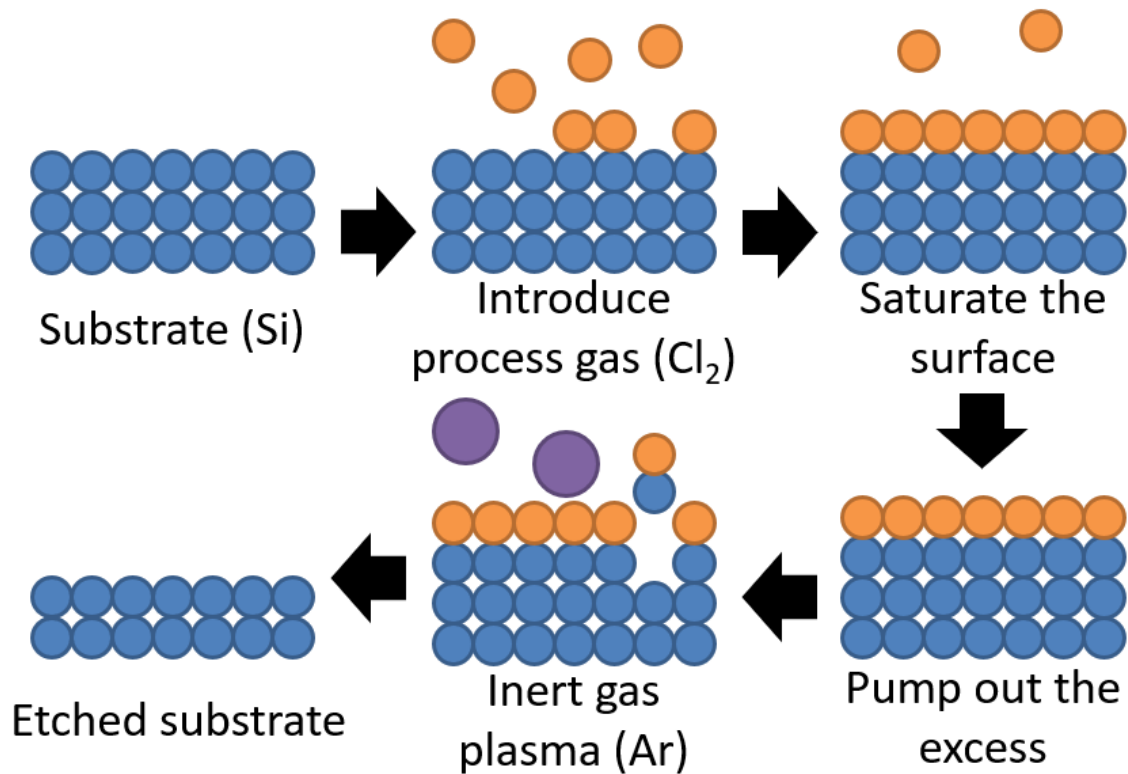


Figure 2.1: Schematic representation of the ALE process.

energy.

The ion energy, dependent on the DC bias, defines three etching regimes in cyclic etching processes - incomplete removal, complete removal and sputtering (see fig. 2.2). In the first one the activated layer was not removed completely, thus, resulting in less etching than expected from an ALE process. The second one - complete removal, which is commonly referred to as the ALE window, features the removal of all activated material and is characterized by its etch rate being independent of ion energy. The last regime represents the case in which the ions have high enough energy to not only remove the activated surface but also physically etch the inactivated material, also known as sputtering.

In an etching tool, ALE can be implemented as a cyclic process with four repeating steps: surface activation, process gas purging (dose purge), plasma-assisted etching (etch step) and etch purge. In the first step the sample is exposed to the process gas selected to modify the surface for long enough so the sample surface is saturated. After the activation, the chamber needs to be purged from the process gas. Then inert-ion plasma is generated and assists etching by supplying the additional energy needed to remove the activated material. The chamber is purged again to ensure no etching products are left in the chamber.

Due to its nature, real or pure ALE is a self-limiting process offering exceptional control of the etching rate and smoothening the sample surface. The self-limiting properties are

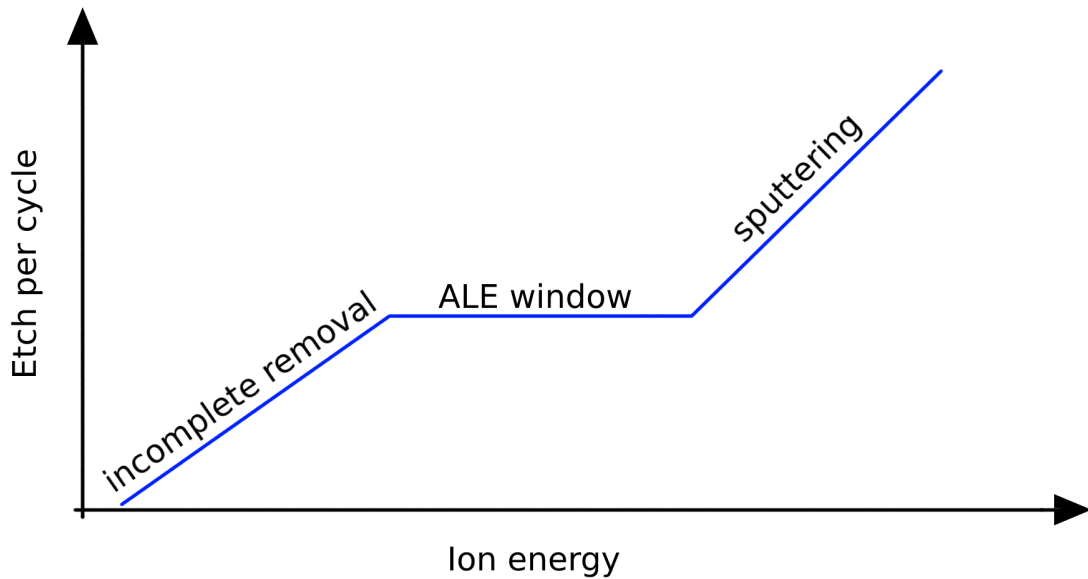


Figure 2.2: Etch per cycle vs. ion energy - representation of the expected dependence in cyclic etching processes. The three parts represent the incomplete removal of the activated surface material, the complete removal or ALE window where the etch per cycle is independent of ion energy, and the sputtering regime.

a result of the fact that the surface needs to be activated in order to be etched, so the etch per cycle grows with etching time until the complete activated surface is etched (every cycle), so there could be no more etching afterwards even if the plasma is present longer. The more common quasi-ALE is a cyclic etching process that features ALE together with other etching processes like sputtering or RIE. That process is quasi self-limiting meaning that the etch per cycle does not saturate but slows down after the activated layer is removed.

In such a process, the first challenge would be finding the right process gas that has the potential to etch the specific material in ALE regime. This would include two main characteristics of the interaction: the gas particles have to lower the energy needed to remove one surface material atom by binding to it and the removed product (most often a process gas particle bound to a material atom) needs to be volatile so it can be easily removed from the chamber avoiding redeposition. Once that has been done, finding the optimal parameters for the surface activation and plasma-assisted etch would be the second one. Derived from the nature of the process, the etch step has obvious optimization criteria in ion energy - not too much to cause additional etching but sufficient to remove the activated layer, and the isotropy of the plasma, defined by the pressure and the DC bias, which depends on the RF power, the activation step parameters are just as important. The process gas needs to be present in a sufficient amount to activate the surface but not in such excess that possible adsorption on other chamber surfaces could

affect the ALE process by introducing process gas at another step via desorption. If any process gas not bound to a material atom is present in the chamber during the etch step, additional activation or RIE could occur and the atomic precision of ALE would be lost resulting in higher etch rate and reduced control. The timing of the activation step should also be just enough to let the activation happen at the specific gas flow and pressure but not to affect other surfaces significantly. In addition, it needs to be purged properly so as little as possible of the process gas is left in the chamber after the purge, ideally, it should be left only on the sample surface and nowhere else.

A possible consequence of having too much process gas is that the gas particles adsorbed to other places in the chamber could desorb during the etch step and get mixed in the plasma, resulting in reactive ion etching if they get ionized, thus, contributing to a higher etching rate than expected and reduced control. Another contribution to the etch rate could be too high radio frequency (RF) power, which results in higher ion energy. If the ions have too high kinetic energy when reaching the substrate, they might initiate sputtering in addition to ALE, thus, further increasing the etch rate.

2.3 Adsorption of Cl_2 on Si(100)

An important factor in the ALE process is the surface coverage of the process gas. In this case, the adsorption of Cl_2 on Si(100) had been previously studied [15] and showed that the dosage and the surface coverage are correlated. The dosage is defined as the product of the gas pressure and the exposure duration and its unit the langmuir signifies the exposure of a surface to a gas with pressure of 10^{-6} Torr for 1 s [16, 17]. At dosage of 2 megalangmuir (ML) the surface coverage approaches its saturation value of 1.0 ± 0.1 monolayers (MLs) for Si(100) surface. At 4 ML, the coverage has already reached saturation. The wafers used in this project were Si(001) but since the crystal lattice of Si is diamond cubic, the planes (100) and (001) are equivalent and there would be no difference in the adsorption process.

Chapter 3

Experimental tools and conditions

The experimental work done for this thesis consists of sample fabrication, cyclic etching, recording and analysis of spectroscopic data, and sample characterization.

3.1 PlasmaTherm ICP-RIE Apex SLR Tool

The cyclic etching processes were performed with the inductively coupled plasma reactive ion etching (ICP-RIE) system Apex SLR from Plasma-Therm LLC (re-branded ICP-RIE Takachi™ [18]). The tool has a main chamber and a load-lock both of which could be pumped down to ultra high vacuum and are connected to a source of N₂ for venting (filling the chamber with gas until atmospheric pressure is reached so the chamber can be opened). They are connected with a door which can be opened so the mechanical arm in the load-lock can transfer the sample in use to the main chamber and back. When a sample is moved by the arm from the load-lock to the main chamber, the sample is placed upon 3 rods that are elevated from the electrode. The sample is then lowered so it lays entirely on the electrode and the rods are level with the surface. The wafer is then clamped with a mechanical clamp. The He backside cooling features a constant He flow through the holes the rods sit in. The He flows from an external source to around the rods, under the mechanical clamp and towards the walls of the main chamber. The clamp has an opening which defined the exposed surface of the wafer. It is a few millimeters smaller, so if the wafer has been displaced from the ideally centered position, the process would still be successful except the exposed surface would be slightly misplaced. If the sample is too far from the ideal position, the He can flow freely into the main chamber and the clamping fails.

The main chamber has two gas inlets at the top - one for venting with N₂ when the main chamber needs to be opened and one for the process gas mixture. The process gas distribution system allows the use of several process gases that are mixed prior to their introduction to the main chamber. The gas flow in each line is individually controlled by a mass flow controller (MFC) and the lines can be purged by nitrogen.

At the bottom of the main chamber is an outlet connected through a throttle valve to a turbo pump and a mechanical pump. At a constant gas flow, the throttle valve position adjusts the operating pressure by changing the pumping speed and is controlled by a capacitance manometer of a membrane-type. The throttle valve position can be expressed numerically with a percentage of the valve open - 0% is completely closed and 100% is completely open. To maintain a stable pressure, the throttle valve position should be stable and instabilities are commonly observed if the position is close to the extremes.

The plasma in this tool can be generated in two ways - by the electrodes or by the ICP coil. The electrodes are practically the plates of a large capacitor and are connected to an RF generator. The RF power creates plasma out of the process gases and the bias induced between the electrodes accelerates the plasma ions towards the sample. Around the top part of the chamber is the ICP coil, which is connected to a similar RF generator and the alternating current through the coil creates plasma throughout the entire space enclosed by the coil.

There are two such tools in Lund Nano Lab - both using O₂, H₂ and Ar as process gases but one also uses Cl-based process gases like Cl₂ and BCl₃, while the other uses F-based ones such as SF₆, CHF₃, CF₄ and C₄F₈, so they are commonly referred to as Cl-Apex and F-Apex respectively. In addition to those process gases, Cl-Apex has CH₄ available while F-Apex has N₂. The Apex tools have parts suitable for 2-, 4-, 6- and 8-inch wafers but the Cl-Apex is usually configured for 2-inch wafers and the F-Apex - for 4-inch wafers. Both are used in fabrication of nanoscale structures by the means of reactive ion etching (see section 2.1). In this project in particular, both were used in sample fabrication (see section 3.3) and the Cl-Apex was used for cyclic etching and development of ALE.

3.2 Cyclic etching process towards atomic layer etching

It has previously been shown that an ALE process can be achieved with an ICP-RIE tool [19], so the main purpose of this project was to attempt the development of ALE for Si with the Cl-Apex tool. The recipe includes the standard loading step and chucking step (during which the He cooling is set up), then a loop featuring a set of 4 steps - surface activation, dose purge, plasma-assisted etching (etch step) and etch purge - repeated in order a set number of times. Finally, the standard dechuck and unloading the sample.

During surface activation Cl₂ is introduced in the chamber in order to adsorb on the Si surface and activate it. The pressure and the flow determine the Cl₂ concentration which together with the step duration or activation time determines the activated surface. For a real ALE process the entire Si surface should be activated, so the activation time needs to be long enough to allow complete activation. However, Cl₂ can adsorb on the chamber walls and other exposed chamber parts and desorb later. If this happens during the etch step, the chlorine molecules may be ionized and the sample may experience reactive ion etching in addition to the ALE, which needs to be minimized. That is the reason why the

activation step should be as short as possible but long enough to allow complete surface activation. To optimize the surface activation, experiments were made with different gas flow, pressure and duration. The etching rate was calculated and the most reasonable parameters were chosen for further experimentation. At this point, the observed process is cyclic etching since the parameters are far from optimal.

The dose purge step is crucial for removing any chlorine left in the gas phase and perhaps desorbing some of the chlorine molecules that has been adsorbed to the chamber surface (including walls and any other completely or partially exposed elements). The only parameter varied in this step was duration and while a shorter purge step would mean much shorter process, since this is the longest step in the recipe, the time needs to be long enough for the excess chlorine in the gas phase to be removed from the chamber. An alternative to the purging step would be pumping - setting gas flow and pressure to 0. One experiment had been done replacing purging with pumping (see section 4.2.1).

The digital etch step is where the Ar plasma provides the additional energy needed for the activated Si layer to be etched. After the optimal parameters of the activation and purging step had been determined, the RF power was varied in order to find the ALE window. Then to find whether the process is self-limiting, the etch step duration (or etch time) was varied.

Finally, the purpose of the etch purge step is to ensure that there are no etching products remaining in the chamber from the etch step. This step has not been changed during this project since there was no reason to suspect its parameters needed optimization.

The cyclic etching process was also performed with varied number of cycles to prove that the etch rate is independent of it. ALE should have etch rate independent of the number of cycles but the same is true for sputtering and reactive ion etching, which are suspected to occur during the etch step of the cyclic etching process. In the end, that could be considered as a confirmation that the tool works properly and no additional etching processes are observed.

3.3 Sample fabrication

The samples used in this thesis were made from Si(100) wafers and used a pattern made with displacement Talbot lithography (DTL)[20] - a photolithography technique in which a highly uniform high-resolution pattern is produced by exposing photoresist to UV light through a grating and moving the sample one period of the resulting interference pattern. The chosen DTL pattern was hexagonally arranged circular holes, which could be transferred by etching or inverted with a lift-off process. There were four types of samples used for the experiments, all of which feature a Si base and a mask on top of it (see fig 3.1): type A - PAR/PMGI two-layer resist mask with holes including an undercut in the PMGI, type B - Cr dots, type C - Cr layer with holes and type D - SiO₂ layer with holes.

Out of the four types of samples used for cyclic etching, only one resulted in a successful

cyclic etching process - the resist mask.

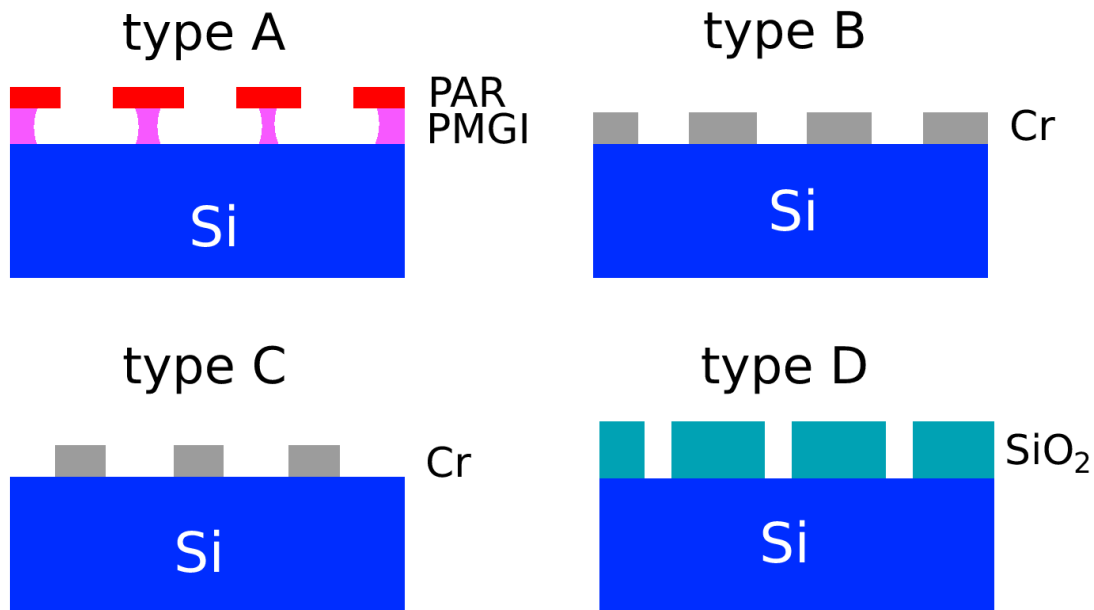


Figure 3.1: Schematic representation of the samples' cross section showing the 4 types of samples used in this project: type A - PAR/PMGI/Si, type B - Cr(solid layer with holes)/Si, type C - Cr(dots)/Si and type D - SiO₂/Si.

3.3.1 Type A - Resist mask

For the fabrication of the resist masked Si samples, a 2-inch Si wafer is heated to 200 °C on a hot plate for 10 min to remove water and other contaminants that may have adsorbed on its surface. Then the wafer is spin-coated with PMGI SF3S, which is typically used as a lift-off resist. The wafer was spun for 45 s at 2000 rpm with an acceleration of 2500 rpm² and post-baked at 200 °C for 10 min. Then the deep UV resist PAR 1085S90 is spin-coated over the previous resist layer for 45 s at 4500 rpm with 2500 rpm² acceleration. The resist was then post-baked on a hot plate for 60 s at 90 °C.

The wafer was then mounted and brought to a safe distance (or separation) of 80 μm from the DTL mask. The wafer was exposed to deep UV light with a wavelength of 193 nm, the source of which is an Ar/F excimer laser. During the exposure the wafer traveled the distance of 8 μm (also known as Talbot range of Talbot distance) periodically until it accumulated the exposure dose 3 mJ/cm². The energy of the laser pulses had been set to 1.5 mJ and their frequency to 100 Hz. The wafer was then baked for 50 s on a hot plate at 90 °C. The resist was immersed in developer MF24A for 60 s, then kept in flowing water for 120 s and dried with N₂. Finally, the wafer was diced into coupons (small chips about 10 mm × 10 mm).

3.3.2 Type B - Cr mask with holes

The fabrication of samples with Cr holes begun with the deposition of 30 nm of Cr on Si wafers, which then underwent 10 min of a dehydration bake at 200 °C on a hot plate. Instead of PMGI, an anti-reflective coating (ARC) ARC162U-308 was spin-coated on the wafers for 45 s accelerated at 2500 rpm² from rest to 2000 rpm. The ARC was then baked for 60 s at 180 °C on a hotplate and the PAR was deposited. The wafers were accelerated to 3000 rpm at a rate of 2500 rpm², spun for 45 s in total, then baked at 90 °C for 60 s.

The samples were exposed to the 193 nm excimer laser light with 3 mJ pulse energy with 100 Hz pulse frequency from an 80 μm separation from the mask. The wafers were moved closer and further away from the mask in a Talbot range of 8 μm until the accumulated dose was 6 mJ/cm². The resist was baked at 100 °C for 50 s. The development featured 60 s immersion in MF24A, followed by 120 s in flowing water and drying with N₂.

The pattern was transferred to the ARC layer and subsequently to the Cr via RIE. The pattern was first etched into the ARC with F-Apex (see section 3.1) by O₂ plasma formed under 15 mTorr pressure with 15 W RF power and O₂ flow of 20 sccm for 20 s. Then the transfer into Cr was done by Cl₂/O₂ plasma with Cl-Apex (see section 3.1) and the following parameters: Cl₂ flow of 20 sccm, O₂ flow of 2 sccm, pressure of 20 mTorr, RF power of 10 W and duration of the etching 8.5 min.

To remove residual organic matter like ARC, the wafer is treated with piranha - a mixture of 3 parts sulfuric acid H₂SO₄ and one part hydrogen peroxide H₂O₂. The process was started with measuring the needed amount of acid in a beaker and heating it to 70 °C. Then the hydrogen peroxide was added and the sample was quickly immersed in the bubbling liquid making sure it was indeed submerged not floating on the surface. The wafer was left there for 10 min, then transferred to a beaker with water for at least 1 min and kept in flowing water for 1 min. After drying it with N₂, the wafer was diced.

3.3.3 Type C - Cr dots mask

The Si samples masked with Cr dots were fabricated from Si wafers using a traditional PMGI lift-off process. Those Si wafers underwent a dehydration bake on a hot plate at 200 °C, then had PMGI spin-coated at 2000 rpm reached at 2500 rpm² acceleration for 45 s and baked for 10 min at 200 °C. Then the photoresist is deposited and spun for 45 s with initial angular velocity of 0 rpm accelerated at the rate of 2500 rpm² until reaching 4500 rpm and maintaining that angular velocity for the remaining spinning time. After being baked at 90 °C on a hot plate for 60 s, the wafers were ready for DTL.

Placed at an 80 μm separation, the wafers accumulated 3 mJ/cm² exposure dose from the excimer laser with 1.5 mJ pulse energy, 100 Hz pulse frequency and 193 nm wavelength. For the duration of the exposure the wafers traveled the 8 μm Talbot distance. After that the resist was baked on a hotplate at 90 °C for 50 s and developed for 60 s in MF24A. The wafer was then kept for 2 min in flowing water and dried with N₂.

To achieve the Cr dots, 30 nm of Cr was deposited over the patterned wafers. They were then placed in beakers with remover 1165 and put on a hot plate at 100 °C for 5 min. Afterward, the beakers were transferred to an ultrasonic bath and were treated three times for 5 s. The wafers were moved to beakers with fresh remover and moved to a hot plate for 5 min at 100 °C. Finally, after being transferred to deionized water for 3 min, the wafers were dried with N₂ and diced into coupons.

3.3.4 Type D - SiO₂ mask

The SiO₂ mask was fabricated from a Si wafer with 225 nm of thermally grown SiO₂ on top using the following recipe[21]. First, the 10 min dehydration bake at 200 °C, then spin-coating the wafer with PMGI SF3S at 1500 rpm with 6000 rpm² acceleration for 45 s and baking it at 200 °C for 10 min, followed by 1 min of thermal relaxation (the sample is left to cool down in air). Afterward, the deep UV resist PAR1085 is spin-coated for 45 s with angular velocity of 2000 rpm reached with the rapid acceleration of 6000 rpm² and baked for 1 min at 90 °C.

The wafer was then exposed to deep UV laser light of 193 nm with pulse frequency of 100 Hz and pulse energy of 1.5 mJ until the accumulated dose had reached 3.5 mJ/cm². The separation was 80 μm and the Talbot range was 8 μm. After the exposure, the resist was baked on a hot plate for 50 s at 100°C and developed in MF24A for 60 s. The wafer was then immersed in flowing water for 2 min before being dried with N₂.

The first step of transferring the pattern to SiO₂ was O₂ plasma ashing to broaden the holes in the resist. This was achieved via RIE with Sirius T2 Plus from Trion Technology. The etching parameters were: O₂ flow of 20 sccm, RF power of 30 W, pressure of 150 mTorr and etch step duration (including plasma ignition) of 30 s. The same tool was then used to transfer the pattern to the thermal oxide with CHF₃ plasma formed at 75 W RF power under 20 mTorr pressure with the flow of CHF₃ being 20 sccm. The etching process took 940 s.

The resist underwent a lift-off process starting with placing the wafer in a beaker with remover 1165 on a hot plate at 100 °C for 5 min. Then the sample was transferred to a beaker with flowing deionized water for 5 min before being dried with N₂. Finally, any resist residues were stripped with Ion Wave 10 microwave plasma system from PVA TePla America with O₂ plasma ashing. The process featured 350 sccm of O₂ and 800 W of MW power.

3.4 Optical emission spectroscopy

Since the ALE process is a sensitive one, the possible contamination from all other processes done in the same chamber should be monitored to assure little or no interference with the ALE. If contaminants are left in the chamber, they would likely be on the chamber surface and may desorb during the cyclic etch poisoning the Si surface and pre-

venting etching or have chlorine adsorbed onto the contaminated surfaces and desorbing later resulting in unwanted RIE. A likely candidate for contaminating the chamber is a process using CH_4 , H_2 and Ar as process gases, since methane is expected to produce some hydrocarbons that could easily adsorb to the chamber surface. The standard way of cleaning the chamber after such process is with O_2 plasma - 50 sccm of O_2 , 5 mTorr pressure, 200 W RF power and 300 W of ICP power. In addition to that, a Cl_2 and Ar cleaning process was tested to determine how effective they are at removing the contaminants. The latter was done with 20 sccm of Cl_2 and 5 sccm of Ar, 5 mTorr pressure, 200 W RF power and 300 W of ICP power. A standard O_2 cleaning was done afterwards.

One possible method of contamination monitoring, that was already available, was optical emission spectroscopy (OES). While there is plasma generated in the chamber, some of the atoms, ions and molecules are in excited state and could relax to a state with lower energy by emitting a photon with a wavelength specific for the transition. Those photons are collected by a photodetector and the plasma spectrum is formed as a representation of the number of photons at small wavelength channels (0.38 nm in width) from 191 to 887 nm collected over a short amount of time (also known as integration time, which was 10 ms for the majority of the experiments, including all cyclic etching ones, and 40 ms for the minority). One recording contains multiple spectra taken over the recording time from the start to reaching an endpoint - a preset event which prompts the software to stop recording the OES data. The endpoint could be given as a set time, e.g. 5 min after the beginning, or until a set threshold has been crossed, e.g. when the average count representation in the region 745 to 755 nm goes under 500 arbitrary units (A.U.) as measured by the spectrometer. The recording can also end when the process step is over, e.g. it can start at the beginning of the etch step and if no set endpoint is reached by the end of it, the recording stops when the step is complete. In addition to being integrated in a recipe, the OES recordings can be done manually requiring a manual start but they can be ended both manually and by reaching an endpoint.

The collected data was analyzed and compared to a database with transitions in the suitable range. While it is expected that some elements would be present, e.g. the plasma gas - atoms, molecules and ions, there are some elements that are unexpected and those are the contaminants. Once they have been determined, the data is analyzed so it follows the time evolution of the plasma peaks and the contaminants' peaks. In a cleaning process, it is expected that the ions and the radicals in the plasma will be consumed in reaction with the contaminants, so their OES signal is weaker in the beginning and increases once a sufficient amount of the contaminants have been cleaned - the increase usually has the shape similar to that of a smoothed step function. The decrease in the contaminants' OES signal happens in a similar way at about the same time. This would indicate that the chamber has been cleaned.

Another use of OES was measuring the average amount of excess chlorine in the etch step during a cyclic etching process. In a pure Ar plasma, there would be no Cl_2 lines in the OES spectrum but the data from the cyclic etching shows precisely that. After the spectra of pure Ar, pure Cl_2 and Cl_2/Ar plasma were obtained, the data was analyzed and the Cl_2 lines that would be used for identification were chosen - 257 nm was the main line

used for identification because there were no overlapping lines and it is certain the signal comes from this line only, in addition, 307 nm was initially chosen as it was separated from the Cl_2 continuum which is the majority of its spectrum. However, 307 had a few other lines nearby resulting in a wide "peak", so most of the time it would give faulty results since the main changes in its intensity would come from the other overlapping lines. To determine comparative Cl_2 quantity, the spectra first had the background removed - either by subtracting the average noise signal found in the recording or using the linear background approximation. In general, removing the average noise signal is the more accurate way since the noise is not exactly linear and if small-intensity peaks are to be measured, such a difference in the background can lead to the wrong intensity (see fig. 3.2). However, since the noise is a bit different for each recording, the linear approximation is necessary for the recordings that have no noise spectra within their data.

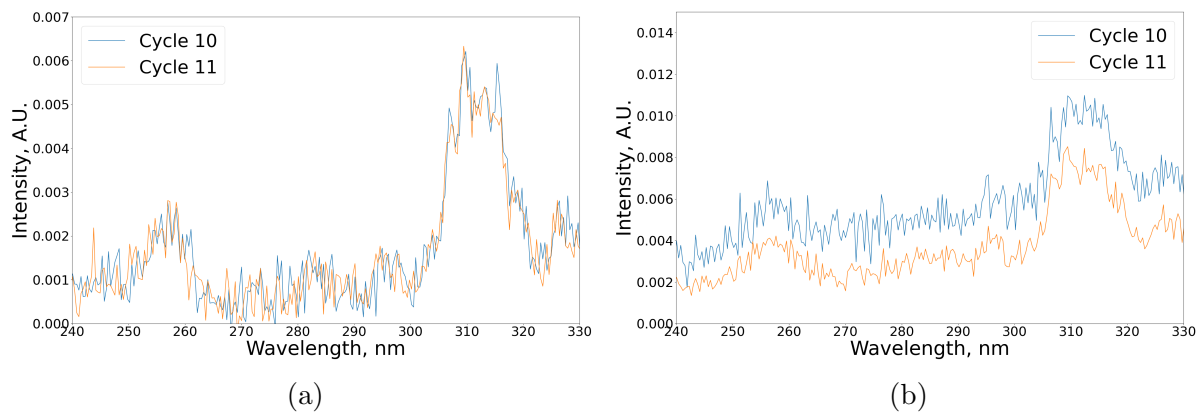


Figure 3.2: Averaged OES spectra of cyclic etching process recording during cycles 10 and 11 with removed background - by average noise signal subtraction (a) and linear background approximation (b).

3.5 Scanning electron microscope

A scanning electron microscope can be used to image samples with features on the nanoscale. The image is formed by an electron beam scanning the sample surface and releasing secondary electrons upon interaction. The beam electrons are generated by an electron gun and collimated by a series of electron lenses (coils). Then they are accelerated towards the sample and when they interact with it the highly energetic beam electron releases electrons from the sample - secondary electrons, which are detected by the secondary electron detectors.

The number of detected electrons depends on the topography and the material content. Surface features affect the secondary electron emission and thus influence the image contrast. The sample material gives additional information to the image since the lighter atoms appear brighter than the heavier ones.

The etching depth measurements after the cyclic etch processes were performed with a SEM. The samples were cleaved and the cleaved edge was imaged with SEM both as a sample cross section and at an angle to show the profile of the etched surface. The sample cross section shows the etched features and allows the etch depth to be measured. The tilted view shows the surface of the features and hint towards surface roughness - it cannot be measured directly with the SEM but if some features within its resolution can be seen, then the surface is probably rough.

Chapter 4

Results and discussions

The ALE process to be developed is a four-step cyclic process done in Cl-Apex. It is used for etching Si with Cl_2 as a process gas activating the surface via chemisorption and Ar ions assisting the removal of the activated layer. The adsorption of Cl_2 is sensitive towards the content of the gas in the chamber, so the gas should be as pure as possible and while the process gas itself is not perfectly pure, the impurities make a very small part of the total gas volume. However, Cl-Apex is a multi-user tool that does feature gases that could lead to contamination, e.g. CH_4 , and if the chamber is contaminated from a previous process, that contamination may affect the ALE process. Moreover, the high etching rate from previous experiments suggests that there may be RIE happening during the material removal step likely due to some Cl_2 left in the chamber after the purging. Therefore, it is crucial to monitor the gas contents and possible contamination, preferably with an in-situ method. This was, in fact, one of the main objectives in this project, the other one being the development of the ALE process itself. The monitoring method used here was optical emission spectroscopy (OES).

To evaluate the etching process, etching rate and relative intensity of Cl_2 are used together with the imaged etching profile. One of the ALE characteristics is that its etch rate is independent of ion energy and thus, DC bias and RF power, so etch rate needs to be measured. In addition, an etch rate that is too high for an ALE process would indicate that there may be another process happening in parallel to the ALE. The relative intensity of Cl_2 is used to estimate the amount of Cl_2 . The etch profile is imaged for measuring the etch depth and to show if there was perhaps something wrong with that particular sample or process run.

4.1 Reference spectra and chamber cleaning

The clamp was changed as a way to reduce contamination and since no OES spectra were taken before the tool was used for etching and it would be certain it has not been contaminated, the best reference spectra available were the ones taken after the clamp

change. The recorded spectra feature pure Ar, pure Cl_2 , Cl_2/Ar and pure O_2 plasma. A comparison with the same spectra taken before the clamp change showed no significant difference (see fig. 4.1).

It was suspected that the $\text{CH}_4/\text{H}_2/\text{Ar}$ etching process used in the Cl-Apex can contaminate the chamber and may need a different cleaning process. That was the reason why the standard O_2 plasma cleaning and an alternative process featuring Cl_2 and Ar were investigated. To test the O_2 cleaning efficiency the processes were done in the following chronological order: standard O_2 plasma cleaning, $\text{CH}_4/\text{H}_2/\text{Ar}$ etching process and standard O_2 plasma cleaning. For the Cl_2/Ar process a similar set of processes was done in the following order: standard O_2 plasma cleaning, $\text{CH}_4/\text{H}_2/\text{Ar}$ etching process, Cl_2/Ar cleaning and standard O_2 plasma cleaning. The OES spectra was recorded for all processes - the first O_2 spectrum would act as a reference and if the process was effective in cleaning the chamber, the same or very similar spectrum should have been observed at the end of the second O_2 process. According to the data, the standard cleaning procedure is enough to remove the contamination accumulated during the CH_4 -based process (see fig. 4.2) while the alternative process seems to increase the contamination (see fig. 4.3). Furthermore, the time evolution of the O_2 peaks and the C_2 and CO peaks, suspected to

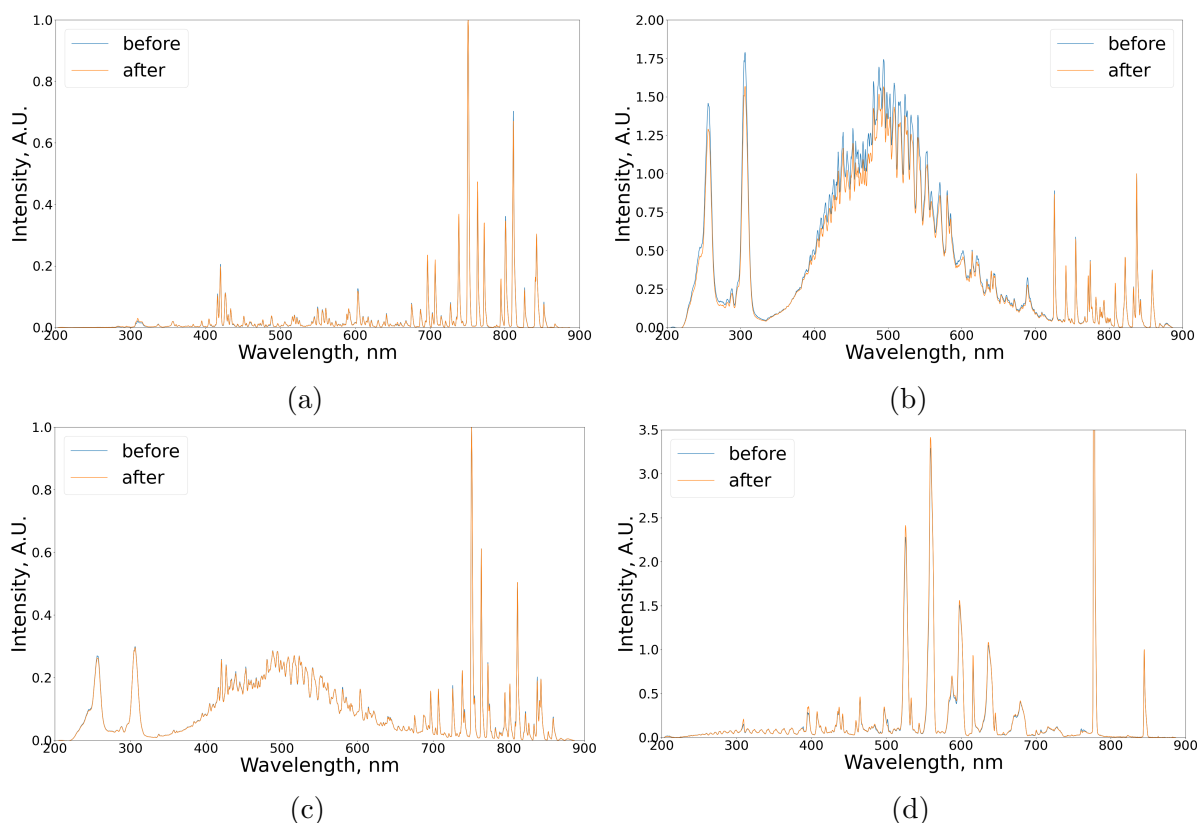


Figure 4.1: OES spectra of Ar (a), Cl_2 (b), Cl_2/Ar (c) and O_2 (d) plasma taken before and after the clamp was changed. All spectra have been normalized to Ar 750 nm (a, c), Cl_2 307 nm (b) or O 844.6 nm (d).

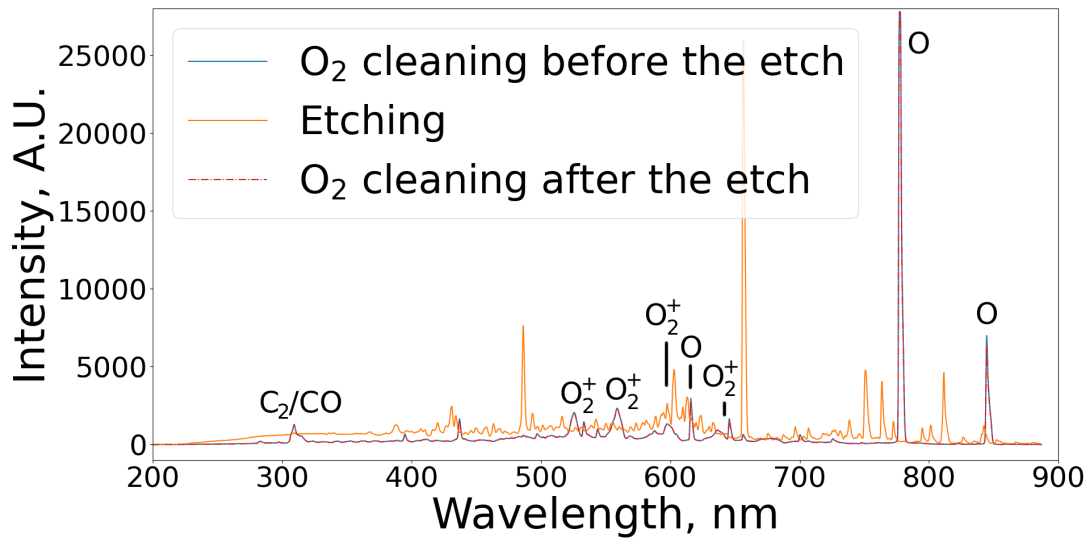


Figure 4.2: OES spectra of the CH₄-based process, the O₂ plasma cleaning before and after the CH₄-based process averaged over the last 5 min (out of 15). All spectra have the background removed but are not normalized.

be the result of hydrocarbon contamination in the chamber, follow the expected intensity change indicating that the chamber is clean (see fig. 4.4, fig. 4.5). Each recording has a slightly different background noise and while the Ar flow is set in the process and should be the same, the spectroscopic measurements may differ slightly, therefore, the spectra are

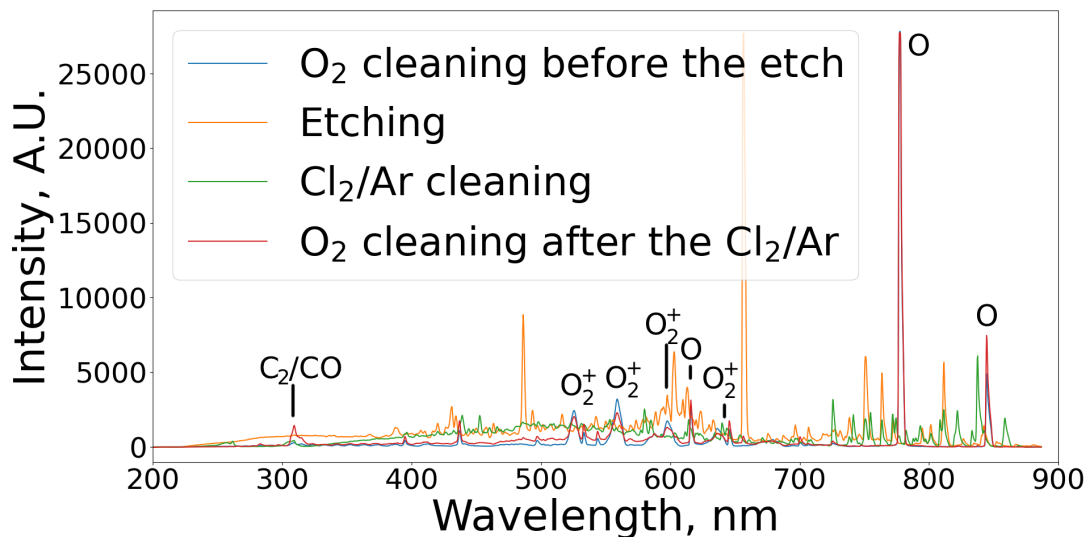


Figure 4.3: OES spectra of the CH₄-based process, the Cl₂/Ar cleaning process, O₂ plasma cleaning before the CH₄-based process and after the Cl₂/Ar cleaning process averaged the last 5 min (out of 15). The background has been removed but the spectra are not normalized.

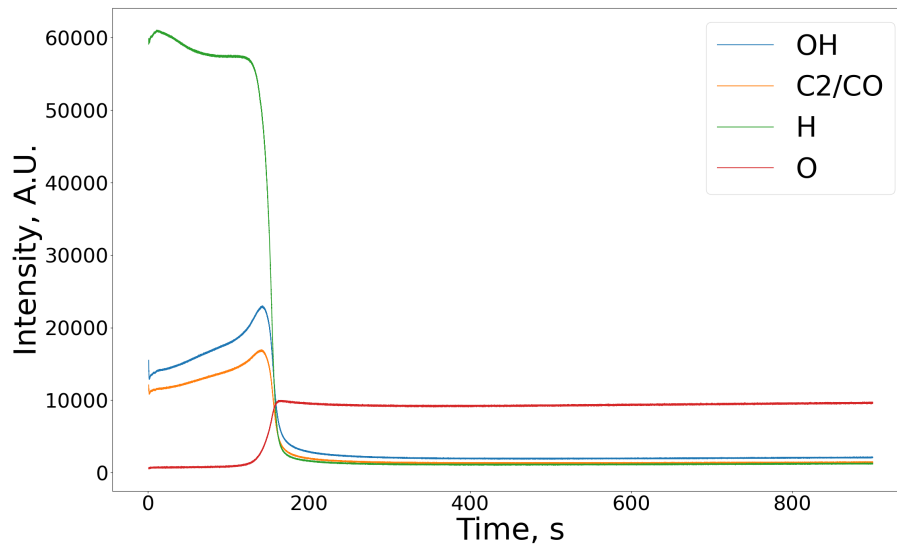


Figure 4.4: Time evolution of selected regions in the spectra (305-312 nm which contains 3 OH peaks, 312-318 nm - C₂ and CO, 655-660 nm - 2 atomic H lines and 843-849 nm - 3 atomic O peaks) during O₂ plasma cleaning after the CH₄-based process.

normalized when presented for more accurate comparison. The OES spectra are always normalized by a line of the used process gas or one of them if multiple ones are used.

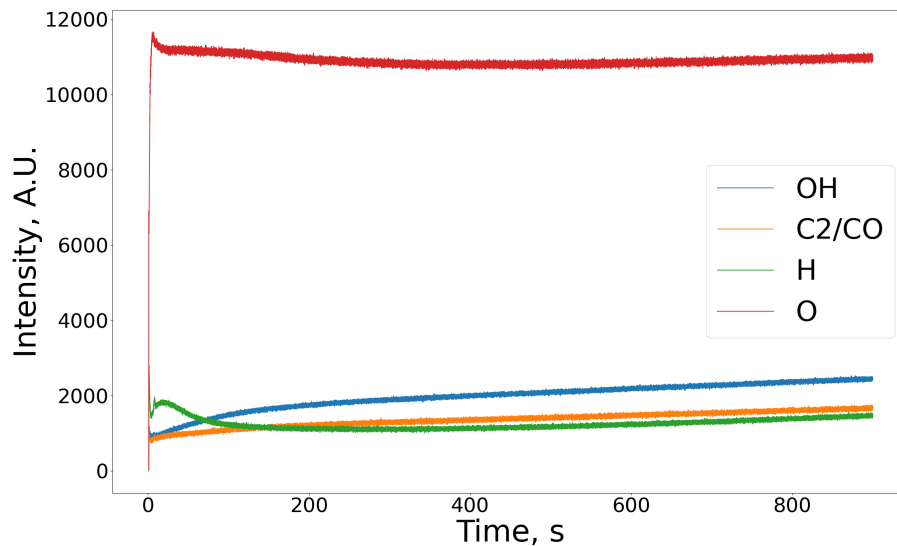


Figure 4.5: Time evolution of selected regions in the spectra (305-312 nm which contains 3 OH peaks, 312-318 nm - C₂ and CO, 655-660 nm - 2 atomic H lines and 843-849 nm - 3 atomic O peaks) during O₂ plasma cleaning after the CH₄-based etching and the Cl₂/Ar cleaning process.

4.2 Cyclic etching process and ALE

An ALE process has been achieved with the Cl-Apex tool before but the problem then was the etch rate that was too high for a real ALE process. However, performing the experiment while skipping activation showed a very low etching rate without Cl_2 and therefore, very little sputtering (see fig.4.6). The team's suggestion was that some of the Cl_2 remains in the chamber and becomes a part of the plasma, thus, resulting in RIE. To minimize the excess Cl_2 while maintaining the ALE requirements, two sets of cyclic etching processes were performed to find the most suitable parameters for a possible ALE process.

The intensity of the Cl_2 257 nm line, relative to the intensity of Ar 750 nm, was used as a measure the relative amount of Cl_2 in the chamber. That was done after the spectra were analyzed and the background was removed, then the area of the peaks (a.k.a. integrated intensity) was calculated and the Cl_2 peak's intensity was divided by the Ar peak's intensity forming the relative integrated intensity of Cl_2 257 nm. This particular Ar line was chosen due to its high intensity - it is the most intense line in the recorded Ar spectra, making it the most suitable choice for normalization and spectrum calibration.

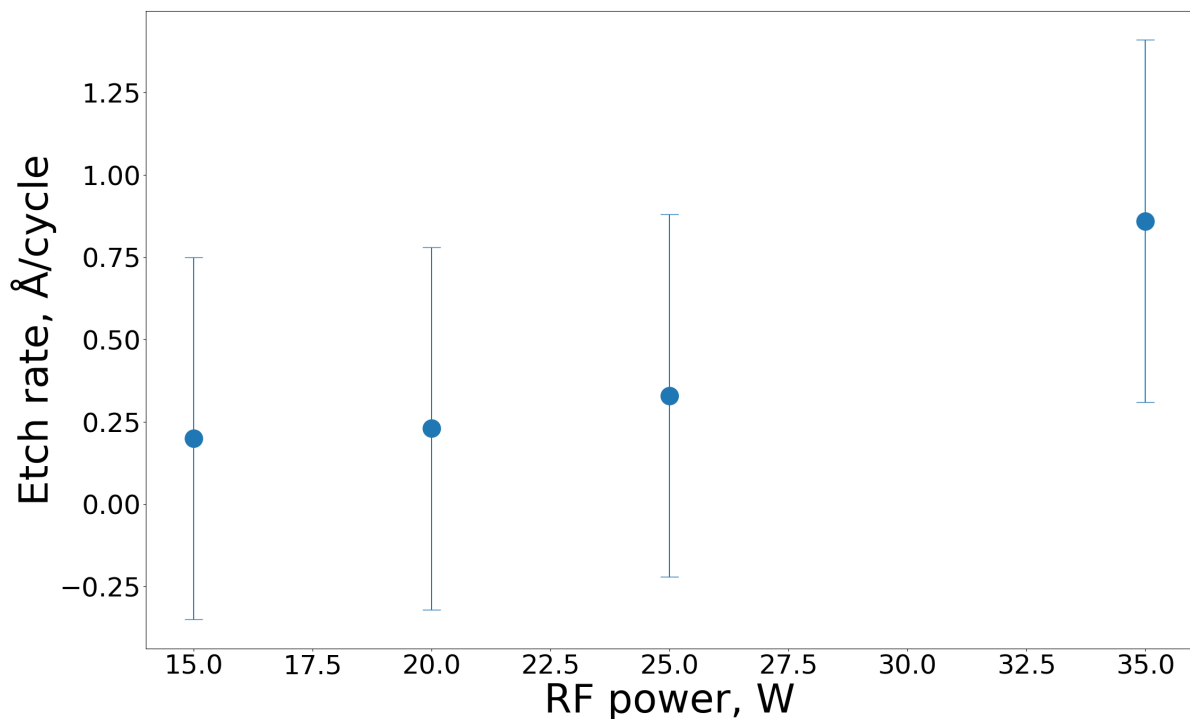


Figure 4.6: Etch rate vs. RF power in cyclic etching with activation step removed (effectively resulting in sputtering of Si). Dose purge parameters: Ar flow of 10 sccm, pressure of 3 mTorr, duration 15 s. Etch step parameters: Ar flow of 10 sccm, pressure of 3 mTorr, duration 10 s. Etch purge parameters: Ar flow of 10 sccm, pressure of 3 mTorr, duration 2 s.

Moreover, since there should be no significant change in the amount of Cl_2 left in the chamber per cycle over the full duration of the cyclic etch process, the spectrum was recorded for the plasma step of the cycles after the parameters have stabilized - 10 and 11, and at the end of the process - 99 and 100 two (except in the set of experiments varying the number of cycles where the last and second to last cycle were used). The recording of two cycles per instance was necessary due to the experiments showing that the plasma ignites at a different time during even and odd cycles which demanded the measurement of one odd and one even cycle for a more accurate comparison.

4.2.1 Activation and Cl_2 purging optimization

The Cl-Apex tool can use several different process gases among which Cl_2 and Ar. During a process, the gas used enters the chamber from an inlet at the top and gets pumped from an outlet at the bottom of the chamber, connected through a throttle valve to the turbo pump. The parameters that can regulate the gas interaction with the sample and can be set by the user are pressure, time and flow. Moreover, if plasma was to be generated, RF power and ICP power can be set by the user and maintained by the system. Since the process used is cyclic etching, the number of cycles can also be altered.

The first set of experiments was focused on the activation step of the cyclic process and the Cl_2 purge time, as well its the alternative - pumping. The investigated parameters in the activation step were the Cl_2 flow, the pressure and the duration of the step. All experiments had a common reference sample (see fig. 4.7) and the parameters were varied one at a time before choosing the optimal conditions for the next set of experiments (section 4.2.2).

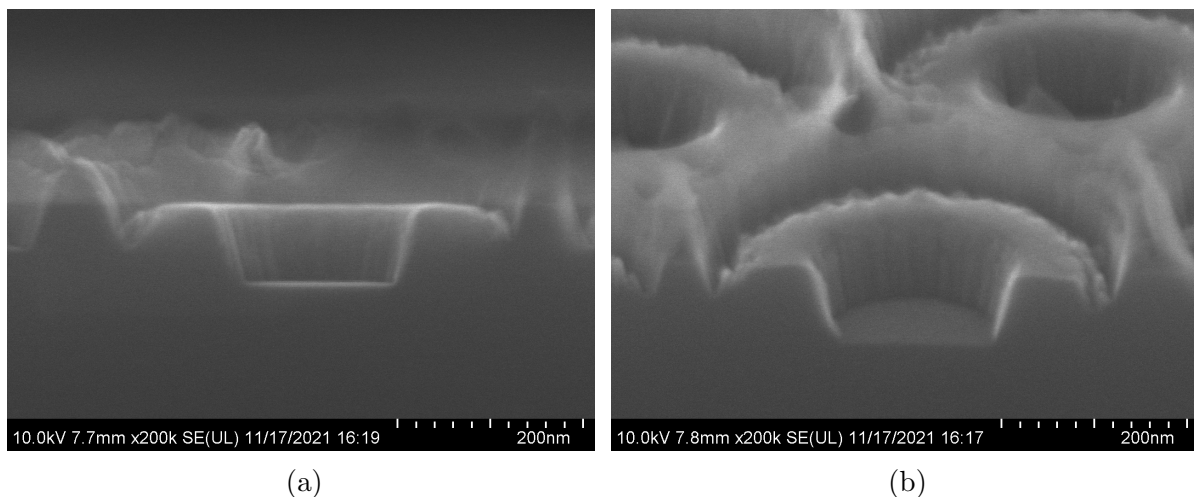


Figure 4.7: Cross section (a) and tilt view (b) of the reference sample for the first set of experiments. Activation step parameters: Cl_2 flow of 20 sccm, pressure of 60 mTorr, duration 20 s. Dose purge parameters: Ar flow of 40 sccm, pressure of 30 mTorr, duration 40 s. Etch step parameters: RF power of 70 W, duration 10 s.

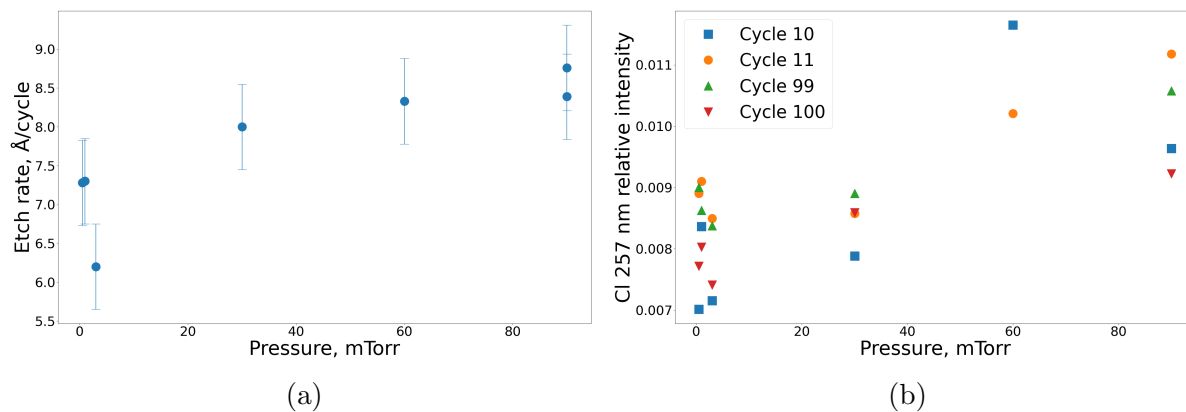


Figure 4.8: Etch rate (a) and relative integrated intensity of Cl_2 257 nm (b) vs. pressure during the activation step. Activation step parameters: Cl_2 flow of 20 sccm, duration 20 s. Dose purge parameters: Ar flow of 40 sccm, pressure of 30 mTorr, duration 40 s. Etch step parameters: RF power of 70 W, duration 10 s.

To determine the etch rate, multiple images like fig.4.7a were taken, the etch depth was measured for every picture and an averaged, then divided by the number of cycles for the etch rate to calculated. The measurement error came from the separate depth measurements, which is 5.5 nm as this is the thickness of the bottom line that appears on fig.4.7a and the like. To calculate the etch rate error a similar technique was used starting with the depth error and dividing it by the number of cycles, which signifies that cyclic etching processes with higher number of cycles would have more accurately measured etch rate.

The expectations were that the etch rate would be independent from the flow, since it does not change the dosage or the concentration of Cl_2 in the chamber unless the conditions are extreme, i.e. the flow is too small for the system to reach the set pressure or too big for the turbo pump to keep the set pressure stable, and increasing for increasing pressure, which results in higher Cl_2 concentration, or step duration, which gives the Cl_2 molecules more time to be adsorbed in the chamber. Both of those etch rate increasing effects are a result of excess Cl_2 left in the chamber after the purge step and likely ionized by the Ar plasma, thus, contributing to RIE, which is affecting the ALE process and should be minimized.

The pressure was varied from 0.5 to 90 mTorr. The data shows increase in etch rate with the increasing pressure with the exceptions of 0.5 and 1 mTorr where the throttle valve position was unstable (see fig.4.8). The lowest stable pressure was 3 mTorr which also resulted in the lowest etch rate among the experiments with varying pressure, thus, being the optimal pressure taking into account the tool's limitations.

The experiments for finding the optimal activation step duration had it ranged from 0.5 to 20 s. An activation time as short as 1 s was sufficient to result in an etch rate of 6.34 Å/cycle (fig.4.9), since 0.5 s showed an instability. In addition, a slight increase in etch rate and Cl_2 257 nm intensity was observed with an increase in the activation time,

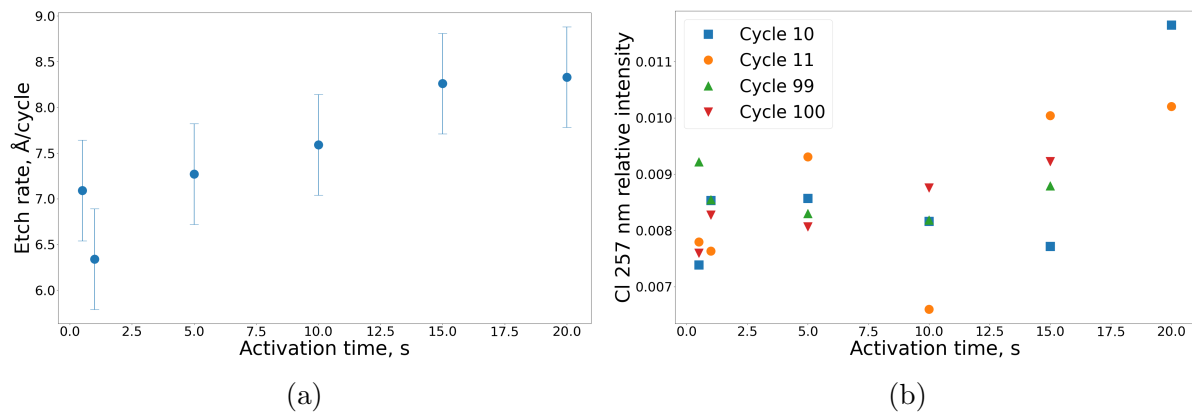


Figure 4.9: Etch rate (a) and relative integrated intensity of Cl_2 257 nm (b) vs. activation time. Activation step parameters: Cl_2 flow of 20 sccm, pressure of 60 mTorr. Dose purge parameters: Ar flow of 40 sccm, pressure of 30 mTorr, duration 40 s. Etch step parameters: RF power of 70 W, duration 10 s.

suggesting that the longer activation step times result in more excess Cl_2 that has remained in the chamber after the purging step.

To examine its effect, the process was performed with Cl_2 flow of 10, 15 and 20 sccm. The results showed little difference between the first and the last experiment in terms of the etch rate and the Cl_2 257 nm relative intensity (see fig. 4.10). However, the experiment done with 15 sccm of Cl_2 showed a deviation from the other two, even though a difference in the flow should not yield a significant differences in the results. A possible explanation for the deviation might be the difference in the properties of the native oxide formed on the Si surface. To remove the oxide-related uncertainties from the experiments, all samples from the following set (section 4.2.2) were treated with HF to remove the native

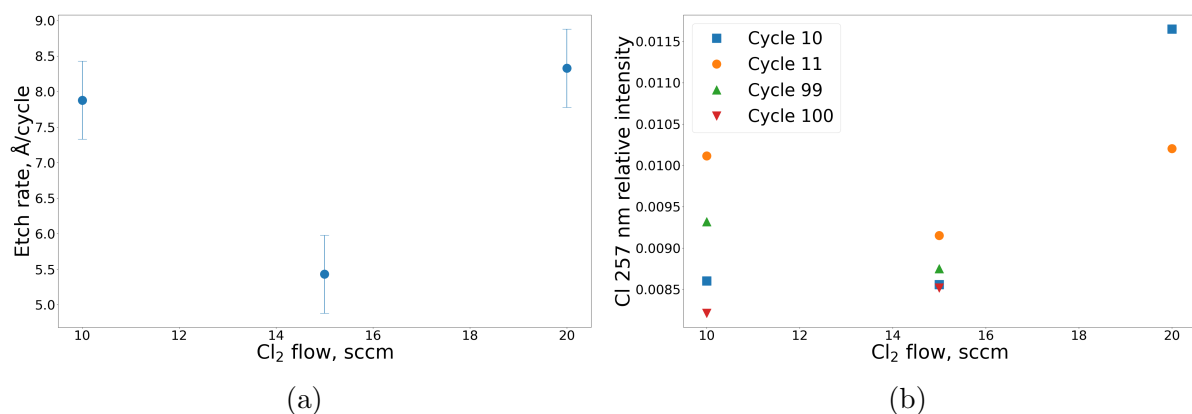


Figure 4.10: Etch rate (a) and relative integrated intensity of Cl_2 257 nm (b) vs. Cl_2 flow. Activation step parameters: pressure of 60 mTorr, duration 20 s. Dose purge parameters: Ar flow of 40 sccm, pressure of 30 mTorr, duration 40 s. Etch step parameters: RF power of 70 W, duration 10 s.

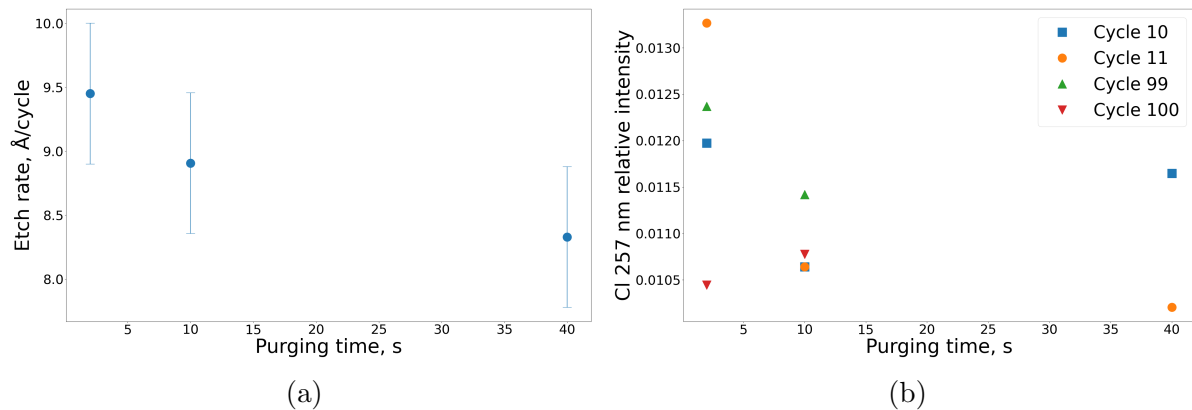


Figure 4.11: Etch rate (a) and relative integrated intensity of Cl_2 257 nm (b) vs. purge time. Activation step parameters: Cl_2 flow of 20 sccm, pressure of 60 mTorr, duration 20 s. Dose purge parameters: Ar flow of 40 sccm, pressure of 30 mTorr. Etch step parameters: RF power of 70 W, duration 10 s.

oxide right before etching. Moreover, to reduce the possible throttle valve instability, the flow of 20 sccm, corresponding to the reference sample, was chosen for the next set of experiments.

The cyclic etch process was performed with a purging step of 2, 10 and 40 s and with the purging step replaced by 40 s pumping. The decrease in purging time resulted in increase in the etch rate (see fig. 4.11) suggesting that the time is not enough to remove the excess Cl_2 from the chamber before the plasma etch step and thus, the 40 s time was chosen as optimal. The pumping resulted in lower etch rate but the OES showed the appearance on N_2 in the chamber, which was likely due to backstreaming of N_2 used in the turbopump. Therefore, this alternative was rejected.

By the end of the first set of experiments, the optimal parameters for the first 2 steps of the cyclic etch process were found to be a Cl_2 flow of 20 sccm, a pressure of 3 mTorr and a duration of 1 s (corresponding to dosage of 3 ML, which results in nearly maximal coverage [15]) for the activation step and a 40 s long purging step. Those parameters were used for all experiments in the next set (section 4.2.2).

4.2.2 Finding the ALE window

After the activation step was optimized, an attempt was made to find the ALE window in terms of RF power and to investigate the typical ALE characteristics (see section 2.2). The first step was varying the RF power from 25 to 60 W and plotting the etch rate dependence on RF power (fig. 4.12a) and looking for the region of complete removal where the etch rate is independent of ion energy (see fig. 2.2) and therefore, independent of RF power. Also, to monitor the amount of Cl_2 , the integrated Cl_2 257 nm intensity relative to the Ar 751 nm was plotted as a function of the RF power (fig. 4.12b) for cycles 10, 11, 99 and 100.

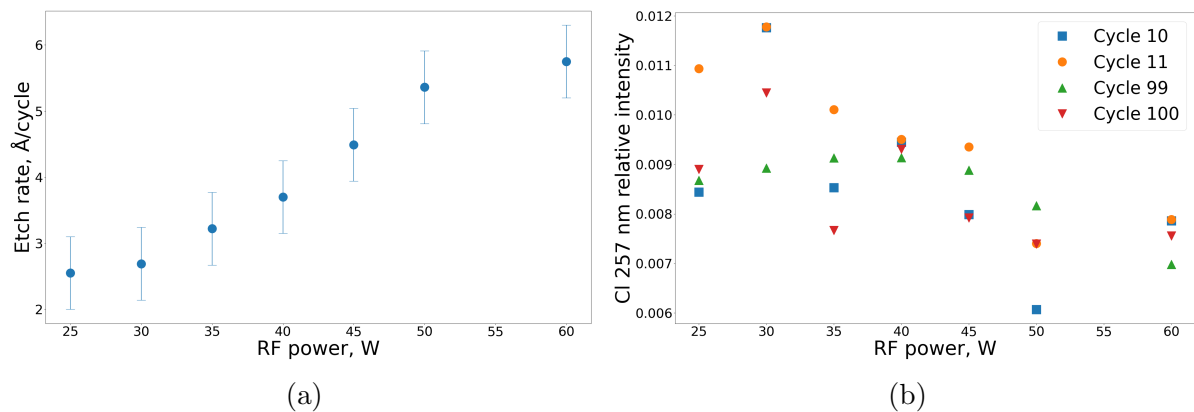


Figure 4.12: Etch rate (a) and relative integrated intensity of Cl_2 257 nm (b) vs. RF power during the plasma step. Activation step parameters: Cl_2 flow of 20 sccm, pressure of 3 mTorr, duration 1 s. Dose purge parameters: Ar flow of 40 sccm, pressure of 30 mTorr, duration 40 s. Etch step parameters: duration 10 s.

From fig. 4.12a, it seems that the ALE regime can be achieved with RF power between 25 and 30 W because the Ar ions have the energy to only remove the activated surface, supported by the low sputtering rate (fig. 4.6). Both samples have a similar profile (see fig. 4.14) with a smooth surface and their etch rates are similar to those previously reported [14].

The process was then performed for different number of cycles since an ALE process should have an etch rate independent of the number of cycles. As expected, the etch rate and Cl_2 257 nm intensity were constant (see fig. 4.13). To better investigate the etch rate dependence on number of cycles, a larger number of cycles should have been used; however, the number of cycles was limited by the mask which was etched by the Ar plasma.

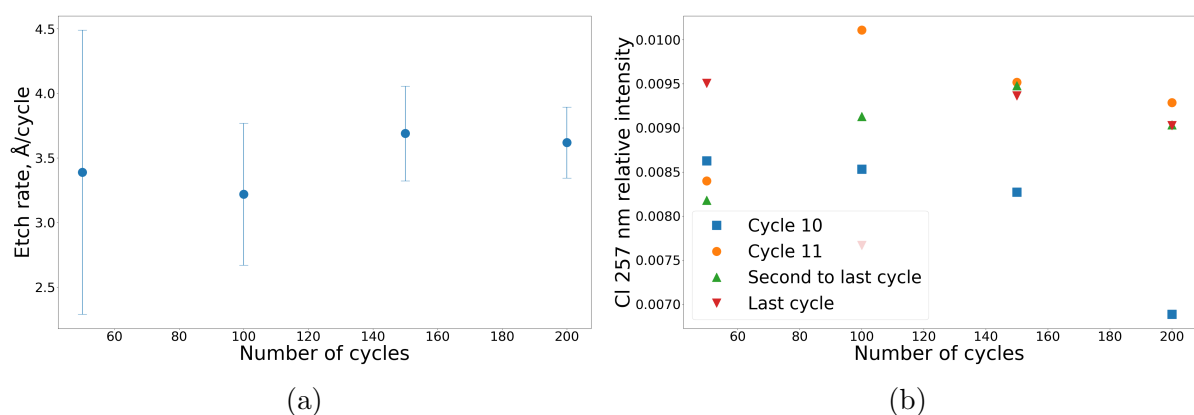


Figure 4.13: Etch rate (a) and relative integrated intensity of Cl_2 257 nm (b) vs. number of cycles. Activation step parameters: Cl_2 flow of 20 sccm, pressure of 3 mTorr, duration 1 s. Dose purge parameters: Ar flow of 40 sccm, pressure of 30 mTorr, duration 40 s. Etch step parameters: RF power of 35 W, duration 10 s.

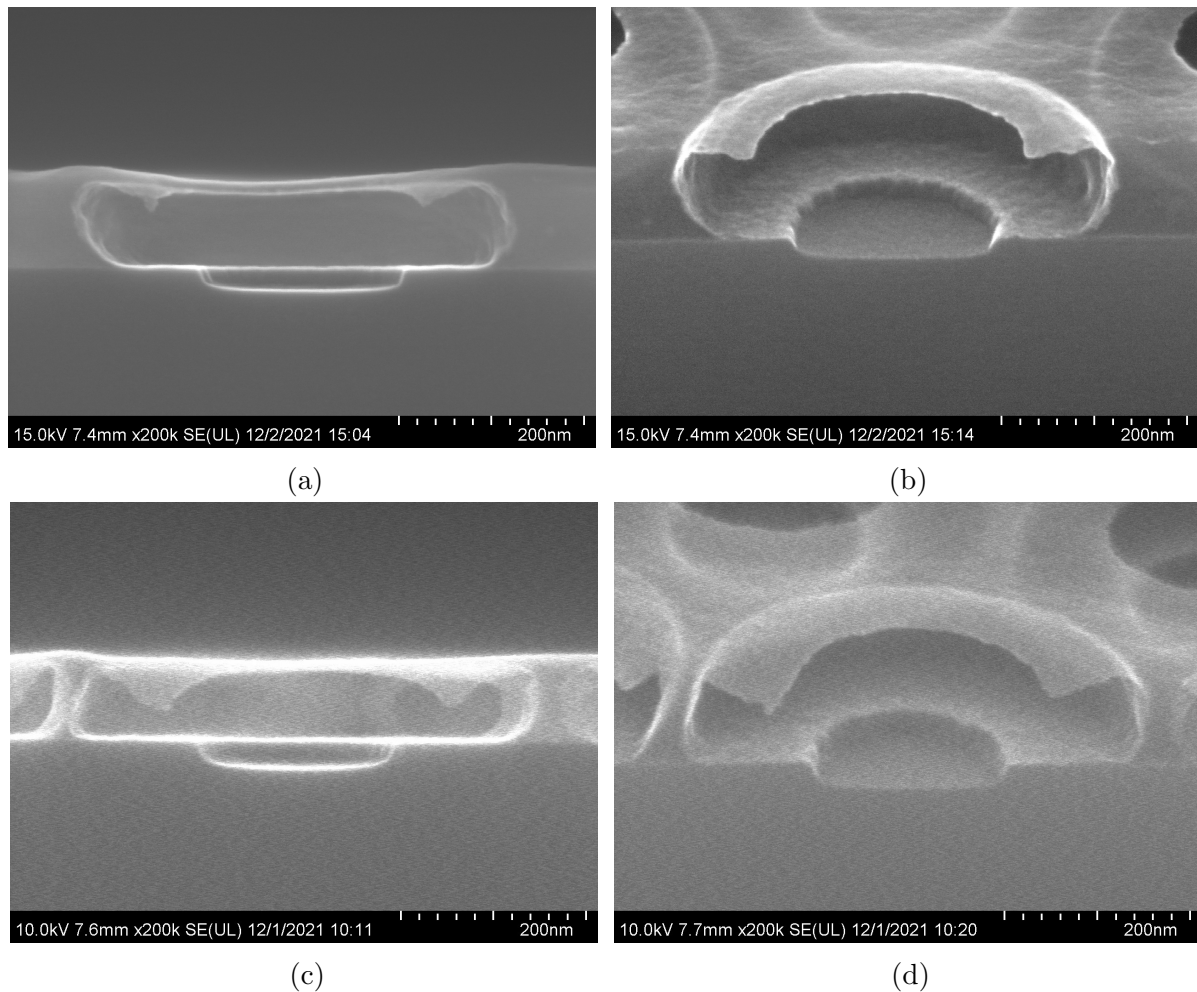


Figure 4.14: SEM image of the cross section (a, c) and 30° tilt (b, d) of the sample processes with RF power of 25 W (a, b) and 30 W (c, d) during the plasma etch step. Activation step parameters: Cl_2 flow of 20 sccm, pressure of 3 mTorr, duration 1 s. Dose purge parameters: Ar flow of 40 sccm, pressure of 30 mTorr, duration 40 s. Etch step parameters: duration 10 s.

After 200 cycles, there was hardly any mask remaining (see fig. 4.15), so further increasing the number of cycles would require a thicker mask or one from a different material that cannot be etched by Ar or has a lower etch rate. It is also important to be noted that sputtering and RIE are also independent of time (or number of cycles), so the conclusion of this set of experiments is that the tool is working properly.

The other important property of an ALE process is the relation between the etch rate and the plasma etch time. If the time is too little for the plasma to remove the complete activated layer, then there would be a linear increase in etch rate until the time is just enough for that to happen. If the time is increased further, no difference in the etch rate should be observed if the process is pure ALE. Otherwise, there might be a linear increase in the etch rate due to sputtering or RIE. In our case, the etch rate increases from 5 to

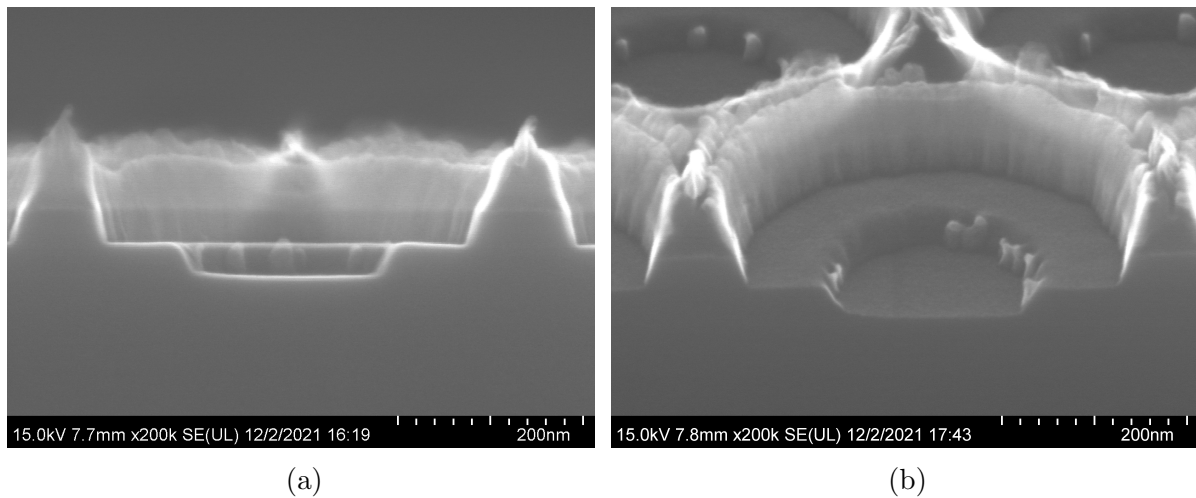


Figure 4.15: SEM image of the cross section (a) and 30° tilt (b) of the sample etched for 200 cycles. Activation step parameters: Cl_2 flow of 20 sccm, pressure of 3 mTorr, duration 1 s. Dose purge parameters: Ar flow of 40 sccm, pressure of 30 mTorr, duration 40 s. Etch step parameters: RF power of 35 W, duration 10 s.

10 s in a linear manner and 12 and 15 s have similar etch rates suggesting that they are in the complete removal regime (see fig. 4.16).

The cyclic processes with this tool would normally result in a pattern of alternating cycles - one where the plasma ignites within 1 s of the beginning of the step and one where the plasma would ignite about 5 s after the beginning. The experiment with 5 s etch time showed a peculiar behavior - during every third cycle, the plasma would not ignite at all, while the other two had the plasma ignited almost immediately, in one of them slightly faster than the other.

The developed quasi-ALE regime could be used in ultra-high resolution patterning. The SEM images (fig. 4.14) of the samples show smooth surface and precisely controlled

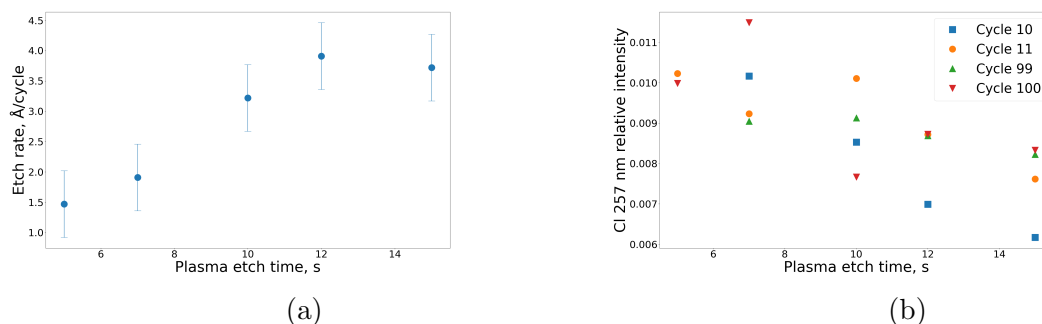


Figure 4.16: Etch rate (a) and relative integrated intensity of Cl_2 257 nm (b) vs. duration of the etch step. Activation step parameters: Cl_2 flow of 20 sccm, pressure of 3 mTorr, duration 1 s. Dose purge parameters: Ar flow of 40 sccm, pressure of 30 mTorr, duration 40 s. Etch step parameters: RF power of 35 W.

etching, both of which are necessary for ultra-high resolution patterning. Even though the samples used in this project were not patterned with ultra-high resolution (smallest openings in the resist mask were about 100 nm), it did demonstrate compatibility by fulfilling the requirements - low highly-controllable etch rate and smooth enough surface to avoid damaging the patterned features.

Chapter 5

Outlook

The OES data was used for monitoring of chamber contamination and amount of excess Cl_2 . The cyclic etching process was optimized to quasi-ALE and while ultra-high patterning has not been demonstrated in this project, the data suggests that this regime would be able to etch structures of the appropriate size with minimal variations in the surface roughness. The samples etched in this regime were patterned with a hexagonal array of circular holes in the resist layer with opening on the order of 100-200 nm showing that even the quasi-ALE regime has sufficient control and precision to etch small features and keep the etched surface smooth. Both of those requirements need to be met for the technique to be applicable in ultra-high resolution patterning.

An unfortunate limitation of the Cl-Apex tool is the long switching time of the components, e.g. the MFCs that control gas content. An upgrade involving faster switching units would improve the accuracy of the measurements. Even though only the duration of the dose purge was investigated in this project, it is possible that the pressure and the Ar flow in this step affect the process so these parameters should be investigated in the future. Moreover, in the cyclic etching processes used in this project OES was recorded only during the etch step since meaningful spectra requires ignited plasma so OES signal (other than background noise) can only be recorded while there is plasma in the chamber. A possible improvement in terms of OES would be to have low-energy ICP on all the time, and record the spectra during the entire cycle - this would make it possible to track the excess Cl_2 including the time of appearance and the reduction of the additional amount of Cl_2 during the dose purge.

In conclusion, the optimization of the cyclic etching process of Si resulted in a quasi-ALE regime combining ALE with sputtering and likely RIE, resulting in an opportunity for ultra-high resolution patterning.

Bibliography

- [1] G.E. Moore. Cramming more components onto integrated circuits. *Proceedings of the IEEE, Proc. IEEE*, 86(1):82 – 85, 1998.
- [2] W.H. Krautschneider, A. Kohlhase, and H. Terletzki. Scaling down and reliability problems of gigabit cmos circuits. *Microelectronics and Reliability*, 37(1):19 – 37, 1997.
- [3] Max N. Yoder. Atomic layer etching, July 1988.
- [4] P.A. Maki and D.J. Ehrlich. Laser bilayer etching of gaas surfaces. *Applied Physics Letters*, 55(2):91–93, 1989.
- [5] Y. Horiike, T. Tanaka, M. Nakano, S. Iseda, H. Sakaue, A. Nagata, H. Shindo, S. Miyazaki, and M. Hirose. Digital chemical vapor deposition and etching technologies for semiconductor processing. In *Journal of Vacuum Science & Technology A (Vacuum, Surfaces, and Films)*, volume 8, pages 1844 – 1850, Dept. of Electr. Eng., Hiroshima Univ., Japan, 1990.
- [6] Chienfan Yu Shwu-Jen Jeng, Wesley C. Natzle. Device and method for accurate etching and removal of thin film. (US5282925A), February 1994.
- [7] Y. Yamamura and K. Tawara. Energy dependence of ion-induced sputtering yields from monatomic solids at normal incidence. *Atomic Data and Nuclear Data Tables*, 62(2):149 – 253, 1996.
- [8] S. Sakurai and T. Nakayama. Adsorption, diffusion and desorption of cl atoms on si(1 1 1) surfaces. *Journal of Crystal Growth*, 237(Part 1):212 – 216, 2002.
- [9] Steven M. George. Thermal atomic layer etching of microelectronic materials. *2021 5th IEEE Electron Devices Technology & Manufacturing Conference (EDTM), Electron Devices Technology & Manufacturing Conference (EDTM), 2021 5th IEEE*, pages 1 – 3, 2021.
- [10] A. Fischer, A. Routzahn, S.M. George, and T. Lill. Thermal atomic layer etching: A review. *Journal of Vacuum Science & Technology A: Vacuum, Surfaces, and Films*, 39(3):030801, 2021.

- [11] P.R. Chalker. Photochemical atomic layer deposition and etching. *Surface and Coatings Technology*, 291:258 – 263, 2016.
- [12] S.G. Walton, D.R. Boris, S.G. Rosenberg, H. Miyazoe, E.A. Joseph, and S.U. Engelmann. Etching with electron beam-generated plasmas: Selectivity versus ion energy in silicon-based films. *Journal of Vacuum Science & Technology A: Vacuum, Surfaces, and Films*, 39(3):033002, 2021.
- [13] Ohori Daisuke, Fujii Takuya, Noda Shuichi, Mizubayashi Wataru, Endo Kazuhiko, Lee Yao-Jen, Tarng Jenn-Hwan, Li Yiming, and Samukawa Seiji. High Electron Mobility Germanium FinFET Fabricated by Atomic Layer Defect-Free and Roughness-Free Etching. *IEEE Open Journal of Nanotechnology*, 2:26 – 30, 2021.
- [14] Park Sang-Duk, Min Kyung-Suk, Yoon Byoung-Young, Lee Do-Haing, and Yeom Geun-Young. Precise depth control of silicon etching using chlorine atomic layer etching. *Japanese Journal of Applied Physics, Part 2 (Letters)*, 44(1A):389 – 393, 2005.
- [15] A. Szabo, P.D. Farrall, and T. Engel. Reactions of chlorine with si(100) and si(111): adsorption and desorption kinetics. *Surface Science*, 312(3):284 – 300, 1994.
- [16] International Union of Pure and Applied Chemistry. *Quantities, Units and Symbols in Physical Chemistry, 2nd edition*. Blackwell Science, Oxford, 1993.
- [17] D. Alpert. New developments in the production and measurement of ultra high vacuum. *Journal of Applied Physics*, 24(7):860 – 876, 1953.
- [18] Plasma-Therm LLC. Takachi icp. http://www.plasmatherm.com/Takachi_ICP.html.
- [19] Md Sabbir Ahmed Khan. Evaluation of atomic layer etching possibility at lund nano lab. Master’s thesis, 2016. Student Paper.
- [20] Konstantins Jefimovs, Lucia Romano, Joan Vila-Comamala, Matias Kagias, Zhentian Wang, Li Wang, Christian Dais, Harun Solak, and Marco Stampanoni. High aspect ratio silicon structures by displacement talbot lithography and bosch etching. 2018.
- [21] Sarah McKibbin. private communication, May 2021.